

# Role of oxygen pressure during pulsed laser deposition on the electrical and dielectric properties of antiferroelectric lanthanum-doped lead zirconate stannate titanate thin films

Yingbang Yao, S. G. Lu, and Haydn Chen<sup>a)</sup>

*Department of Physics and Materials Science, City University of Hong Kong, Kowloon, Hong Kong*

Jiwei Zhai

*Functional Materials Research Laboratory, Tongji University, Shanghai, People's Republic of China*

K. H. Wong

*Department of Applied Physics, The Hong Kong Polytechnic University, Kowloon, Hong Kong*

(Received 4 November 2003; accepted 10 April 2004)

Lanthanum-doped lead zirconate titanate stannate antiferroelectric thin films of  $\sim 420$  nm with compositions in the antiferroelectric tetragonal region have been prepared on Pt-buffered Si substrates by pulsed laser deposition. Effects of oxygen pressure during deposition were studied, with emphasis placed on the electrical and dielectric properties of the films. The dielectric constant and the maximum polarization increased with the oxygen pressure during deposition, from 75 to 125 mTorr. So did the dielectric strength. This property enhancement with deposition oxygen pressure was believed to be due to the reduction of pyrochlore phase in the films. However, increasing the oxygen pressure beyond 150 mTorr during deposition had led to the increase of surface roughness, which eventually resulted in film cracking. It was also found that increasing the oxygen pressure did not benefit the fatigue performance in any appreciable way. © 2004 American Institute of Physics. [DOI: 10.1063/1.1758312]

## I. INTRODUCTION

Lead-based antiferroelectric ceramics have been investigated for many years, due to their promising applications in actuators<sup>1</sup> and high-energy storage capacitors.<sup>2</sup> This class of materials has good dielectric and ferroelectric characteristics.<sup>1-5</sup> As demanded by the miniaturization of microelectronic devices, thin-film form of such materials has been prepared by means of various deposition techniques such as sol-gel,<sup>3-5</sup> pulsed laser deposition,<sup>6</sup> etc. La-doped and Nb-doped lead zirconate stannate titanates (PLZST or PNZST) are two materials which received wide attention of late. Effects of processing parameters on properties of these materials have been undertaken, such as sintering temperature,<sup>3</sup> postdeposition annealing temperature,<sup>3</sup> thickness effects,<sup>4-5</sup> etc. Pulsed laser deposition (PLD) method is well known for its accurate composition control; it has been used for thin-film growth of oxide superconductors,<sup>7</sup> ferroelectric/antiferroelectric ceramics<sup>6,8-10</sup> among other types of metallic and inorganic materials. The ambient gas during deposition in the PLD process has been found to affect the films in many aspects, such as stoichiometry,<sup>7</sup> texture,<sup>6,9-11</sup> microstructure<sup>8</sup> as well as electrical/dielectric performance of the films.<sup>8,10</sup> Usually, oxygen is introduced during deposition in order to suppress lead-loss as well as to reduce oxygen vacancies in the films, which are a very common issue for the fabrication of lead-based (anti-)ferroelectric<sup>12</sup> thin films. With increasing oxygen pressure

during deposition, the preferred orientation could change, for example, from *a* axis preferred orientation to *c* axis preferred orientation. Moreover, the properties of the films could be improved due to the suppression of oxygen vacancies. On the other hand, the surface roughness becomes an issue with increasing oxygen pressure, which will deteriorate the film when more and more droplets are present in the film. Consequently, an optimized processing route needs to be developed to reach an appropriate level of trade-offs.

Many efforts have been attempted, from the viewpoint of device applications, to investigate the relationship between oxygen vacancies and fatigue,<sup>13</sup> leakage current<sup>6</sup> in the films. For the PLZST/PNZST antiferroelectric materials, there are fewer reports about the oxygen pressure effects, via the PLD process, on properties or microstructures of the films. In this paper, the effects of oxygen pressure during deposition on the microstructure, electrical/dielectric/ferroelectric properties of antiferroelectric PLZST thin films have been studied.

## II. EXPERIMENT

Lanthanum-doped lead zirconate stannate titanate tetragonal antiferroelectric ceramic target, with the nominal composition of  $\text{Pb}_{0.97}\text{La}_{0.02}(\text{Zr}_{0.65}\text{Sn}_{0.28}\text{Ti}_{0.07})\text{O}_3$ , was prepared by the conventional solid-state reaction method. 5 mol % excess of Pb was adopted to compensate for the lead loss during processing. The calcination temperature was 800 °C and calcination duration was 4 h, while the sintering temperature and duration were 1200 °C and 2 h, respectively. The x-ray diffraction (XRD) patterns of the target showed a pure perovskite phase.

<sup>a)</sup> Author to whom correspondence should be addressed; electronic mail: aphchen@cityu.edu.hk

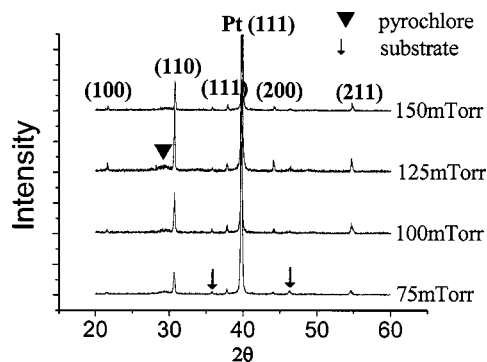


FIG. 1. XRD patterns of the films deposited under different oxygen pressure from 75 to 150 mTorr.

A two-step approach was adopted: PLD of thin films followed by a postdeposition annealing. The 248 nm KrF excimer laser, operated at the repetition rate of 10 Hz, was used to ablate the target. The laser density irradiated on the rotating PLZST target was about  $6 \text{ J/cm}^2$ . Details of the PLD equipment configuration and parameters were previously published.<sup>11</sup> The substrate temperature during deposition was kept at  $200^\circ\text{C}$ . The oxygen pressure during deposition was varied from 75, 100, 125 mTorr to 150 mTorr and the deposition duration was accordingly varied from 14.7, 12.5, 11.1 min to 10 min in order to keep the thickness of all samples approximately the same. Postdeposition annealing process was performed at  $650^\circ\text{C}$  for 30 min in a horizontal tube furnace with oxygen flow. A SIMENS D-500 x-ray powder diffractometer equipped with a  $\text{Cu } K\alpha$  radiation source was used to identify the crystallographic structures of the samples while the surface morphology was observed by field-emission scanning-electron microscopy (SEM) (JOEL JSM-6335F). The film thickness was obtained from the SEM cross-section images.

After postdeposition annealing, gold pads with the area of  $0.0314 \text{ mm}^2$  were deposited onto the films by DC sputtering to serve as the top electrodes for electrical measurements. Dielectric properties were obtained first from room temperature up to about  $400^\circ\text{C}$  using a HP 4284A LCR meter. This was repeated a few times to ensure reproducible results. Other ferroelectric properties, such as  $P$ - $E$  and  $C$ - $V$  curves, were measured as well at various temperatures using a RT66 ferroelectric tester from Radiant Technology. The excursion of samples to high temperatures ( $\sim 400^\circ\text{C}$ ) also served the purpose of improving the interface between the Au electrode and PLZST films, thus giving reliable results on electrical and leakage current properties.

### III. RESULTS AND DISCUSSIONS

#### A. Crystallographic phase and microstructure

Figure 1 shows the x-ray diffraction patterns taken at room temperature from the PLZST films prepared under different deposition oxygen pressure; all were subjected to postdeposition annealing at  $650^\circ\text{C}$  for 30 min. All samples showed a powder diffraction pattern with the strongest peak at  $2\theta$  angle of about  $30.7^\circ$ , denoted as (110) Bragg reflection peak. The full width at half maximum (FWHM) of the (110)

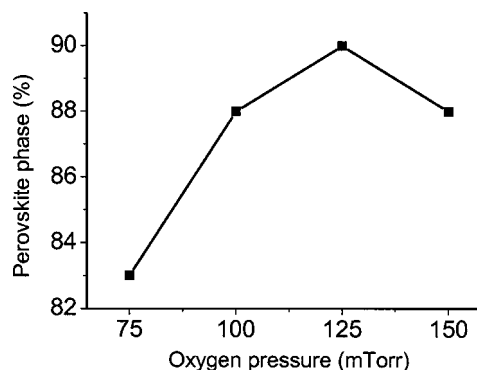


FIG. 2. Volume percentage of perovskite phase of the films deposited under different oxygen pressures, calculated from the XRD results.

peak ranges from  $0.22^\circ$ ,  $0.18^\circ$ ,  $0.16^\circ$  to  $0.16^\circ$  for the samples under deposition oxygen pressure of 75, 100, 125, and 150 mTorr, respectively. The corresponding grain sizes calculated using the Scherrer equation were 27, 33–37 nm with increasing oxygen pressure. There was no observable dependence of preferred orientation on the deposition oxygen pressure, contrary to the previous studies.<sup>6,9–11</sup> The reason was attributed to the two-step process (a low substrate temperature deposition followed by a high temperature postdeposition annealing) instead of in situ growth in the previous reports. Thus, the effects of deposition rate, strains, etc., which are closely related with the deposition oxygen pressure known to affect the lattice parameters and orientation of the film pronouncedly,<sup>10</sup> could be minimized. Nevertheless, the oxygen pressure during deposition did have significant effect on the electrical properties, which will be discussed in the following sections.

There exists a small bump at about  $29.6^\circ$  in the XRD results for all samples shown in Fig. 1, which is the (222) Bragg reflection peak from a pyrochlore phase. This observation implies that all the films are not of pure perovskite phase but with a small fraction of pyrochlore phase. This is probably due to the lead loss during the annealing process and hence the lead-deficient or oxygen-deficient pyrochlore phase formed. The relative volume percentage of the pyrochlore to the perovskite phases may be qualitatively estimated by comparing the intensity of the major x-ray diffraction peaks of the pyrochlore and perovskite phases, which are (222) and (110), respectively. Therefore, the volume percentage of the perovskite phase was estimated by Eq. (1),

$$\% \text{ Perovskite} = \frac{I_{\text{Perov}}(110)}{I_{\text{Pyro}}(222) + I_{\text{Perov}}(110)} \times 100. \quad (1)$$

It has been shown<sup>14</sup> previously that this simplified estimation provides a good agreement with more rigorous quantitative x-ray analysis methods. This is a commonly adopted method to outline a relative change of volume fraction in a two-phase system. The estimated perovskite contents in the films deposited under different oxygen pressures are shown in Fig. 2, which indicates an increase from 83% to 90% as the deposition oxygen pressure increases from 75 to 125 mTorr, then drops at 150 mTorr.

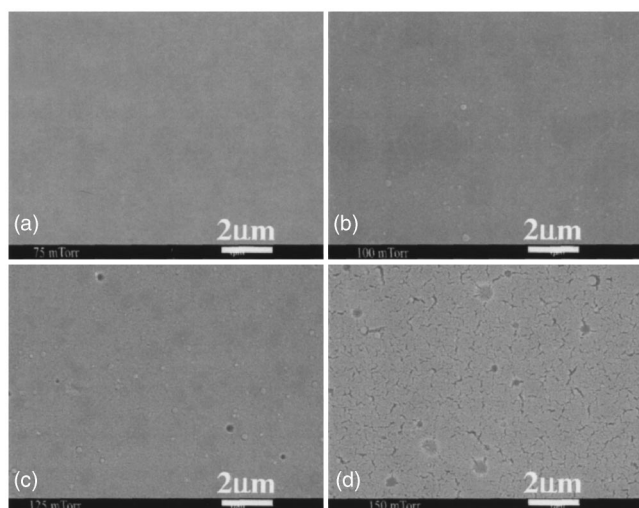


FIG. 3. SEM plane view of the films deposited under the oxygen pressure of (a) 75 mTorr, (b) 100 mTorr, (c) 125 mTorr, and (d) 150 mTorr.

The surface morphology of the samples is shown by the SEM micrographs in Fig. 3. The surface roughness increased with oxygen pressure, so did the amount of particulates on the surface. This was a common phenomenon for the PLD process.<sup>8</sup> The origin of the particulates comes from multiple sources. During deposition at high oxygen pressure, small clusters ablated from the target have a high probability of condensation in oxygen gas because of the formation of the shock front typical of the PLD process, resulting in large clusters. During and/or after the condensation of the clusters, they probably lose their energy, or heat, leading to “cool” clusters on the substrate. These clusters then deposit randomly on the substrate and surface migration/diffusion hardly occurs due to insufficient energy. These clusters are normally spherical with the dimension in nanometer range.<sup>15</sup> On the other hand, high oxygen pressure will increase the confinement of the plasma ejected by the laser pulse incident onto the target surface.<sup>16</sup> Thus the energy density is increased. Consequently, the particulates originated from splashing of molten droplets most likely occur when the transfer of laser energy into heat occurs at a faster rate than is needed to evaporate a mass volume of depth equal to half the skin depth. The size of such particulates is in the micron and sub-micron range and these particulates are irregular in shape.<sup>15</sup>

These two kinds of particulates formed from the vapor state or liquid ejecta seemed to show the same trend with the gas ambient during deposition, which accounted for the increase of surface roughness as well as the amount of particulates in the films when the deposition oxygen pressure was increased. Moreover, as the deposition oxygen pressure increased to 150 mTorr, the film included many cracks as shown in Fig. 3(d), which were not observed in the films deposited at lower oxygen pressures. These wormlike cracks could be ascribed to the release of gas bubbles, which were trapped into the film deposited at low temperature, during postdeposition annealing.<sup>17</sup> Since at high oxygen pressure in a PLD process, more particulates were introduced into the film as described above, there would be more pores and

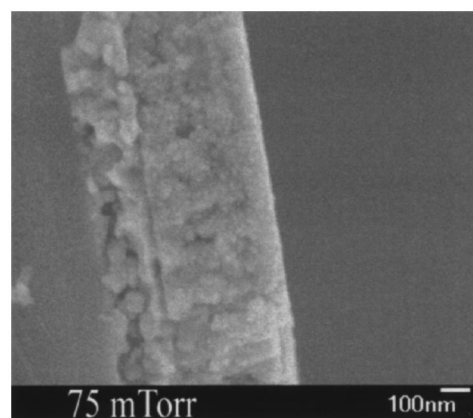


FIG. 4. SEM cross-section view of the film deposited under the oxygen pressure of 75 mTorr.

openings in the films, which could easily absorb gas atoms from the ambient during deposition at a low temperature. These trapped gases were released during postdeposition annealing, thus leading to the formation of large cracks.

The cross-section view of a sample prepared at 75 mTorr is illustrated in Fig. 4. The thickness of the sample is around 420 nm. Another point that needs to be noted from the cross-section SEM view is the interdiffusion between Pt and Ti. The interface between these two layers is not clearly defined, which indicates that the Ti atoms could have diffused into the Pt layer through the Pt grain boundaries and reacted with oxygen to form Ti oxide when the film was annealed at high temperature<sup>18</sup> in oxygen ambient. The oxygen supply for the reaction may be from the film, thus leading to the oxygen vacancy formation in the film, or from the ambient gas.

## B. Electrical and dielectric properties

The polarizations versus electrical field ( $P$ - $E$ ) hysteresis loops are delineated in Fig. 5. These measurements were carried out at the frequency of 10 kHz. All the films showed “slanted” hysteresis loops and some remanent polarization, which were believed to be due to the retention of ferroelectric phase after the field was removed.<sup>18</sup> Field-induced AFE-FE switching was demonstrated by the appearance of a ferroelectric loop at higher field strengths. The saturated polarization was from 7.5, 12.0  $\mu\text{C}/\text{cm}^2$  to 17.5  $\mu\text{C}/\text{cm}^2$ , as the deposition oxygen pressure increased from 75, 100 mTorr up to 125 mTorr. However, when the deposition oxygen pressure was further raised to 150 mTorr, the saturated polarization drastically decreased to about 2.5  $\mu\text{C}/\text{cm}^2$  and the polarization hysteresis loop was suppressed. The electrical field corresponding to the phase transition between the antiferroelectric (AFE) and the ferroelectric (FE) phase was about 114 and 200 kV/cm for FE to AFE (backward switching) and AFE to FE (forward switching), respectively, for all the films except those prepared at 150 mTorr. This was because the excessively high oxygen pressure during deposition deteriorated the crystal structures and hence the ferroelectric and dielectric properties were degraded.<sup>8</sup>

Nevertheless, a moderately high oxygen pressure of 125 mTorr was necessary to grow high quality PLZST films as

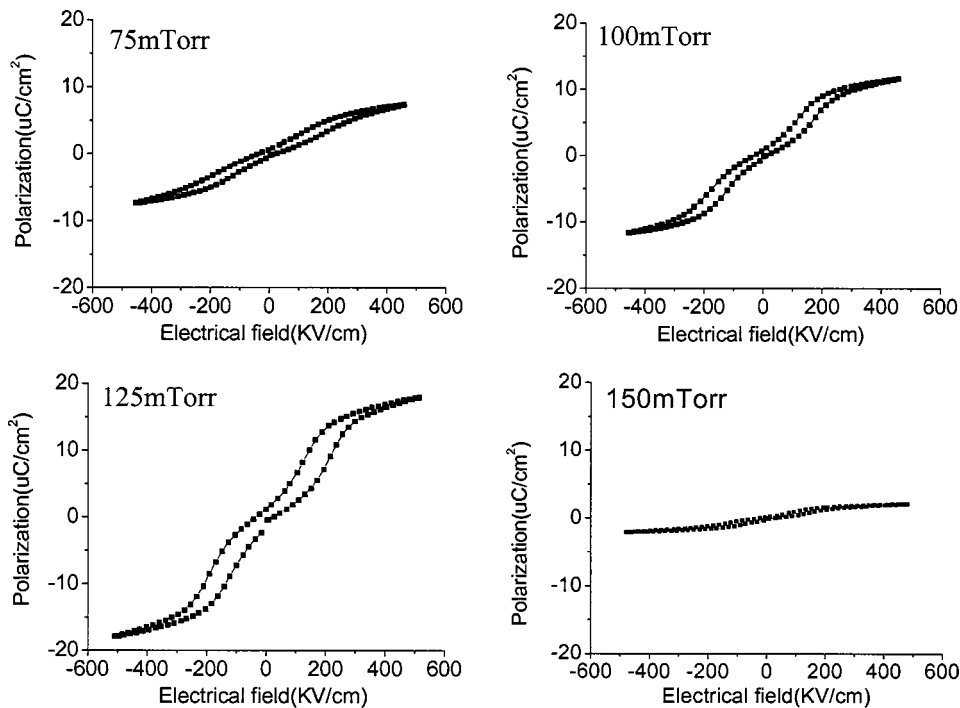


FIG. 5.  $P$ - $E$  hysteresis loops of the films deposited under oxygen pressure from 75 to 150 mTorr.

shown above. This could be explained in terms of effects related to the incorporation of oxygen into the films as a result of collisions between the ejected plasma and ambient oxygen gas.<sup>15</sup> Sufficient oxygen supply under sufficiently high oxygen pressure could preserve the lead fraction by forming  $PbO$ , whose vapor pressure is lower than that of  $Pb$ , on the growing surface.<sup>12</sup> On the other hand, for films deposited at low temperature followed by a high temperature post-deposition annealing, growth kinetics of perovskite phase was limited by the nucleation rate of the crystallites and the nucleation of crystallites took place at the bottom substrate.<sup>17,20</sup> These nucleated "seed" perovskite grains on the film/substrate interface grew through the film to the free surface and the fluorite or pyrochlore phase, which is an intermediate phase formed at low temperature, could first form before transforming into the perovskite phase.

However, due to  $Pb$  deficiency in case of lower oxygen pressure during deposition, this intermediate fluorite or pyrochlore phase might not fully transform to the perovskite phase because  $Pb$  deficiency would stabilize the fluorite or pyrochlore phase.<sup>20</sup> Incomplete transformation to the perovskite phase results in the degradation of the ferroelectric properties as well as dielectric properties. It is obviously necessary to prevent lead loss during processing in order to eliminate the second phase.<sup>19,20</sup> Therefore, for films deposited under lower oxygen pressure, e.g., 75 mTorr, the incompleteness of phase transformation due to the lead loss probably accounted for the inferior dielectric and ferroelectric performance.

Figures 6 and 7 illustrate the frequency and temperature dependence of dielectric constant and dielectric loss. Films deposited under higher oxygen pressure, 125 and 150 mTorr, showed low frequency dielectric relaxation: the dielectric constant and dielectric loss decreased with frequency, from 658 to 252, 243 to 213 and from 0.56 to 0.03, 0.82 to 0.02,

for the 125 and 150 mTorr sample, respectively, under the frequency ranging from 100 Hz to 1 MHz, as shown in Fig. 6. Since higher deposition oxygen pressure produced films with higher surface roughness, there were more defects, which could accommodate space charges between the film and the substrate. The space charge accumulation in the interface region could lead to the formation of a low resistance layer connected in series with the near-insulating dielectric

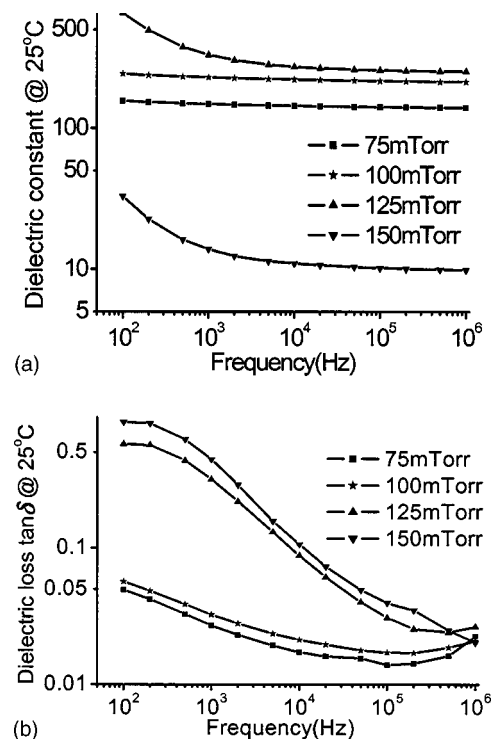


FIG. 6. Frequency dependence of dielectric constant (a) and dielectric loss (b) in a log-log plot at room temperature.



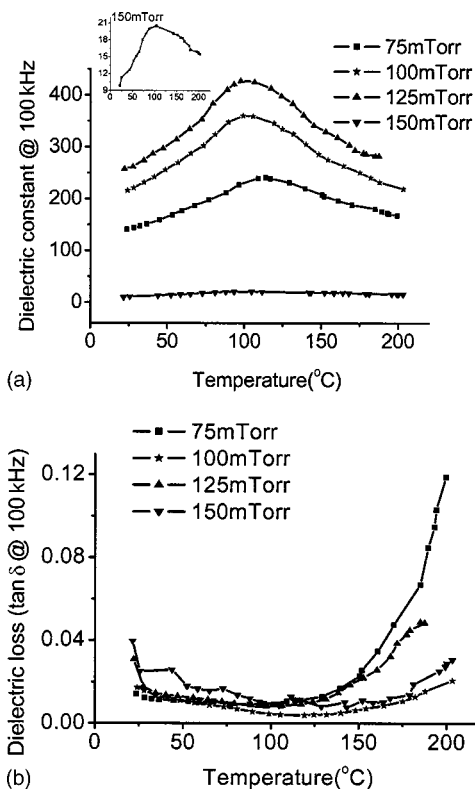


FIG. 7. Dielectric constant (a) and dielectric loss (b) against temperature at 100 kHz. The inset in (a) is the  $K$ - $T$  curve of a 150 mTorr sample on an enlarged scale.

film. Such a system could be well described by the Maxwell-Wagner two-layer model,<sup>21</sup> which reveals the dielectric relaxation and high loss under low frequencies. For the films deposited under relatively low oxygen pressure, 75 and 100 mTorr, the dielectric constant remained almost constant around 150 and 220 with frequency, respectively, and the dielectric loss was lower than 0.06 throughout the frequency range from 100 Hz to 1 MHz.

The dielectric constant increased with oxygen pressure during deposition except for the 150 mTorr sample. The Curie temperature, which corresponds to the phase transition between the antiferroelectric and the paraelectric phase, was about 100°C as indicated by the dielectric maximum in the temperature dependence of dielectric constant curves in Fig. 7. However, the film deposited under 75 mTorr oxygen pressure showed a little deviation of the Curie temperature from 100°C to 110°C, which could be attributed to the incompleteness of perovskite phase formation under lower oxygen pressure or due to the stress effects,<sup>22</sup> etc. The inset in Fig. 7(a) shows the temperature dependence of dielectric constant for the film deposited at 150 mTorr oxygen pressures. Though the dielectric constant was very small compared to those of the others, it nevertheless showed an obvious dielectric peak at about 100°C. The dielectric loss showed a weak decrease with the measurement temperature up to 100°C and then increased dramatically, which could be resulted from the thermally activated ionic conduction mechanism.<sup>21</sup>

The leakage currents of the samples were measured as a function of dc voltage as shown in Fig. 8. Since the bipolar

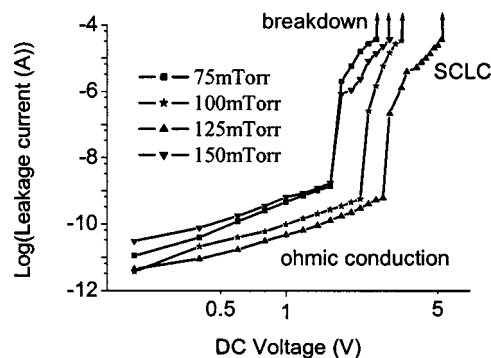


FIG. 8. Leakage currents under different DC voltage in a log-log plot. The electrode area is  $3.14 \times 10^{-4}$  cm<sup>2</sup>. SCLC is for space charge limited conduction.

response time was not more than 1 ms, the leakage currents were taken after the samples experienced different voltages for 10 s. Under low field, the Ohmic conduction mechanism dominated the leakage current, the magnitude of which decreased with oxygen pressure during deposition from 75 to 125 mTorr then increased again at 150 mTorr. The breakdown voltages followed a similar trend, going from 2.5 to 3.2 V then to 5 V with 75, 100, and 125 mTorr oxygen pressure, then returning to about 2.8 V at 150 mTorr. (All samples had similar thickness of  $\sim 400$  nm.) A fairly sharp jump from Ohmic conduction to seemingly the space charge leakage current effect<sup>6</sup> took place before the final breakdown. The onset field for the hypothesized space-charge-limited conduction (SCLO) was different for different film conditions (38, 52, and 67 kV/cm for the 75/150, 100, and 125 mTorr sample, respectively). It must be noted that due to breakdown, the SCLC effect at high field could not be easily substantiated. The fact that the jump from Ohmic conduction to the hypothesized SCLC effect was quite sharp (about two orders of magnitude) could imply that a "soft" breakdown might have occurred before the final breakdown.

Another property, which needs to be considered seriously from the viewpoint of practical applications, is the fatigue performance of the films under a switching electrical field. It has been suggested that the fatigue in antiferroelectric ceramics is much less severe than that of ferroelectric.<sup>23</sup> It is possibly due to the fact that in the switching of the antiferroelectric phase, the polarization direction changed by 180° with the consequent smaller internal stresses than the 90° domain switching of in ferroelectrics.<sup>23,24</sup> The antiferroelectric films had very small values of switchable polarization as compared with those of the ferroelectric films due to the antiparallel configuration of the dipoles in the antiferroelectrics. Therefore, the saturated polarization ( $P_s$ ) and remanent polarization ( $P_r$ ) were adopted to represent the fatigue property of the antiferroelectric films.

Figure 9 shows the normalized  $P_s$  and  $P_r$  (normalized with respect to the  $P_s$  before fatigue) of the PLZST thin films deposited under various oxygen pressures. The normalized  $P_s$  decreased but  $P_r$  increased with increasing number of cycles. The relative decrease of  $P_s$  after  $5 \times 10^9$  switching cycles was 38%, 28%, and 23% for the films deposited under 75, 100, and 125 mTorr oxygen pressure. It shows that the

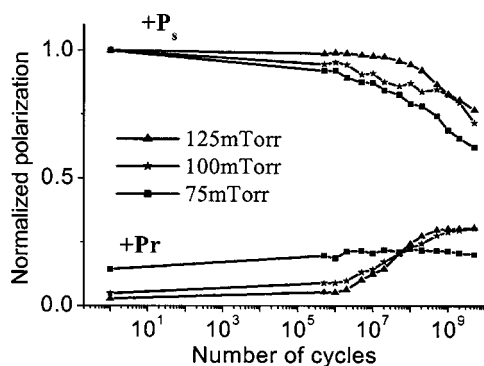


FIG. 9. Normalized saturated polarization and remanent polarization of the films deposited under the oxygen pressure of 75, 100, and 125 mTorr after different number of switching cycles.

films deposited under higher oxygen pressure were more stable. The decrease of  $P_s$  was suggested to come from the defect dipoles or pinned-domains, which could not return to the initial state of antiparallel alignment after switching for many cycles.<sup>24</sup> Since high oxygen pressure was required to keep the stoichiometry of the Pb-based antiferroelectric/ferroelectric films, films deposited under lower pressure would introduce more defects (cation and anion vacancies) into the films. Therefore, the domain pinning would be more serious in the films deposited under lower oxygen pressure and hence the higher fatigue rate of  $P_s$ .

The change of  $P_r$  was not seen to depend on the deposition ambient in a regular fashion, which was from 0.14 to 0.20, 0.05 to 0.31 and 0.02 to 0.31 for the 75, 100, and 125 mTorr samples. The normalized remanent polarization of the 75 mTorr sample was relatively larger than those of the other samples. The origin of the larger remanent polarization in the 75 mTorr sample was probably due to the domain pinning,<sup>23,24</sup> which could be caused by defects in the films, such as oxygen/lead vacancies. Likewise the increase of the  $P_r$  in all these samples was probably due to the domain pinning, which mostly occurred in the near-electrode region due to migration of the oxygen vacancies to the film-electrode interface during switching.<sup>13,23,24</sup> Another possible explanation for the increase of the  $P_r$  was the decrease of film resistivity<sup>23</sup> with increasing number of cycles and consequently, the leakage current would increase. Because the integrity of leakage current with time would be considered to be polarization by the hysteresis tester (RT66 from Radiant Tech.), the polarization would increase with leakage current.

#### IV. CONCLUSIONS

The optimum oxygen pressure during the pulsed laser deposition of PLZST thin films was found to be in the range

of 100–125 mTorr. With increasing oxygen pressure, the roughness of the films increased and so did the dielectric constant and the saturated polarization. Leakage current and fatigue were also found to decrease with the oxygen pressure during deposition. However, excessively high oxygen pressure during deposition would destroy the film and degrade the performance of the film greatly. Low-frequency dielectric dispersion was observed for the samples deposited under higher oxygen pressure, which was caused by the space charge in the interface between the film and the substrate.

#### ACKNOWLEDGMENTS

This work was supported in full by a HK RGC grant (Grant No. CityU 1049/02E) via the City University of Hong Kong (CityU). The authors would like to acknowledge the technical assistance from T. F. Hong and Daniel Yau of CityU.

- <sup>1</sup>W. Y. Pan, Q. Zhang, A. Bhalla, and L. E. Cross, *J. Am. Ceram. Soc.* **72**, 571 (1989).
- <sup>2</sup>W. Y. Pan, C. Q. Dam, Q. M. Zhang, and L. E. Cross, *J. Appl. Phys.* **66**, 6014 (1989).
- <sup>3</sup>B. Xu, L. E. Cross, and D. Ravichandran, *J. Am. Ceram. Soc.* **82**, 306 (1999).
- <sup>4</sup>B. Xu, Y. Ye, Q.-M. Wang, and L. E. Cross, *J. Appl. Phys.* **85**, 3753 (1999).
- <sup>5</sup>Z. Jiwei, M. H. Chung, Z. K. Xu, X. Li, and H. Chen, *Appl. Phys. Lett.* **81**, 3621 (2002).
- <sup>6</sup>S. S. N. Bharadwaja and S. B. Krupanidhi, *J. Appl. Phys.* **86**, 5862 (1999).
- <sup>7</sup>A. Gupta, *J. Appl. Phys.* **73**, 7877 (1993).
- <sup>8</sup>T. Nakamura, Y. Yamanaka, A. Morimoto, and T. Shimizu, *Jpn. J. Appl. Phys., Part 1*, **34**, 5150 (1995).
- <sup>9</sup>X. S. Gao, J. M. Xue, J. Li, C. K. Ong, and J. Wang, *Microelectron. Eng.* **66**, 926 (2003).
- <sup>10</sup>Y. Ding, J. Wu, Z. Meng, H. L. Chan, and Z. L. Choy, *Mater. Chem. Phys.* **75**, 220 (2002).
- <sup>11</sup>W. Wu, K. H. Wong, C. L. Mak, C. L. Choy, and Y. H. Zhang, *J. Appl. Phys.* **88**, 2068 (2000).
- <sup>12</sup>A. Masuda, K. Matsuda, Y. Yonezawa, A. Morimoto, and T. Shimizu, *Jpn. J. Appl. Phys., Part 2* **35**, L237 (1996).
- <sup>13</sup>J. F. Scott and M. Dawber, *Appl. Phys. Lett.* **76**, 3801 (2000).
- <sup>14</sup>J. Chen, A. Gorton, H. M. Chan, and M. P. Harmer, *J. Am. Ceram. Soc.* **69**, C303 (1986).
- <sup>15</sup>D. B. Chrisey and G. K. Hubler, *Pulsed Laser Deposition of Thin Films* (Wiley, New York, 1994), p. 167.
- <sup>16</sup>R. K. Singh and J. Narayan, *Phys. Rev. B* **41**, 8843 (1990).
- <sup>17</sup>V. Stankus, J. Dudonis, L. L. Pranevicius, D. Milcius, and C. Templier, *Thin Solid Films* **426**, 78 (2003).
- <sup>18</sup>H.-J. Nam, D.-K. Choi, and W.-J. Lee, *Thin Solid Films* **371**, 264 (2000).
- <sup>19</sup>S. S. Sengupta, D. Roberts, J.-F. Li, M. C. Kim, and D. A. Payne, *J. Appl. Phys.* **78**, 1171 (1995).
- <sup>20</sup>M. J. Lefevre, J. S. Speck, R. W. Schwartz, D. Dimos, and S. J. Lockwood, *J. Mater. Res.* **11**, 2076 (1996).
- <sup>21</sup>D. O'Neill, R. M. Bowman, and J. M. Gregg, *Appl. Phys. Lett.* **77**, 1520 (2000).
- <sup>22</sup>N. A. Pertsev, V. G. Koukhar, R. Waser, and S. Hoffmann, *Appl. Phys. Lett.* **77**, 2596 (2000).
- <sup>23</sup>Q. Y. Jiang, E. C. Subbarao, and L. E. Cross, *J. Appl. Phys.* **75**, 7433 (1994).
- <sup>24</sup>J. H. Jang, K. H. Yoon, and H. J. Shin, *Appl. Phys. Lett.* **73**, 1823 (1998).